

Electronic Supplementary Information (New Journal of Chemistry)

Can Surface Capping Ligands Probe Cation Exchange in Inorganic Nanoparticles?

Saoni Rudra,¹ Madhumita Bhar,¹ Prasun Mukherjee^{1,*}

Centre for Research in Nanoscience and Nanotechnology, University of Calcutta, JD-2,

Sector-III, Salt Lake, Kolkata-700106 West Bengal, India

E-mail: pmcrnn@caluniv.ac.in, pmukherjee12@gmail.com

Table S1. A Summary of Characterization Methods Employed for Cation Exchange.

Reactant	Cations Added	Product	Characterization Technique ^a	Reference
CdSe	Ag ⁺ Excess Cd ²⁺ to Ag ₂ Se	Ag ₂ Se CdSe	UV-visible, PL, XRD, TEM	¹
CdS	Ag ⁺	CdS-Ag ₂ S	TEM, EDS, XRD	²
CdS	Cu ⁺	Cu ₂ S	PL, TEM, EFTEM, XRD, VASP Simulation	³
InAs	Cu ²⁺ Ag ⁺ Au ³⁺	InAs/Cu InAs/Ag InAs/Au	TEM, XRD, XPS, UV, PL, ICPAES, STM, STS	⁴
ZnSe	Cd ²⁺ , Cu ²⁺ Cd ²⁺	Cu:Zn _{1-x} Cd _x Se Cu:Zn _{1-y} Cd _y Se	UV-visible, PL, TEM, XRD, ICP-AES	⁵
ZnS	Hg ²⁺ Ag ⁺ Pb ²⁺	HgS Ag ₂ S PbS	UV-visible, PL, XRD, EDS, TEM, SEM	⁶
ZnS	Pb ²⁺ Hg ²⁺	PbS HgS	XRD, TEM, ICP-MS	⁷
CdSe	Ag ⁺	CdSe/Ag	UV-visible, PL, XRD, TEM, ICP-OES, ICP-MS	⁸
CdS CdSe CdSSe alloy	Ag ⁺ Cu ⁺	CdS/Ag, CdS/Cu CdSe/Ag, CdSe/Cu CdSSe/Ag, CdSSe/Cu	XRD, EDS, TEM, XPS, XANES, EXAFS	⁹
CdSe ZnS	Ln ³⁺ [Ln = Pr, Nd, Sm, Eu, Tb, Dy, Ho, Er, Tm, Yb]	CdSe/Ln ZnS/Ln	UV-visible, PL, FTIR, TEM, EDS	¹⁰
Zn(Tb)S	M ⁿ⁺ [M ⁿ⁺ = Pb ²⁺ , Hg ²⁺ , Cd ²⁺ , Ca ²⁺ , Mg ²⁺ , Na ⁺ , K ⁺]	Zn(Tb)S/M	UV-visible, PL, XRD, TEM, EDS	¹¹
Zn(Tb)S	Cd ²⁺	Zn _{1-x} Cd _x (Tb)S	UV-visible, PL, FTIR, XRD, TEM, EDS	¹²
Cd ₃ As ₂	Ga ³⁺	GaAs	UV-visible, TEM, XRD	¹³
CdSe/CdS	Cu ⁺	Cu _{2-x} Se/Cu ₂ S	UV-visible, XRD, TEM, HAADF-STEM	¹⁴
CdSe	Cu ⁺ Zn ²⁺ to Cu _{2-x} Se	Cu _{2-x} Se ZnSe	UV-visible, PL, TEM, XRD	¹⁵
Cu ₂ Te	Cd ²⁺	CdTe	UV-visible, PL, TEM, HAADF-TEM, XPS, EDS, XRD, FFT, ICP-OES	¹⁶
Cu _{2-x} Se	Sn ⁴⁺ Sn ²⁺	Cu ₂ SnSe ₃ SnSe	UV-Vis-NIR, TEM, RAMAN, XRD, ICP	¹⁷
ZnS	Mn ²⁺	ZnS/Mn	UV-visible, PL, TEM	¹⁸
CdS	Cu ²⁺	Cu _x S (x = 1-2)	UV-visible, PL, EPR	¹⁹
CdSe	Al ³⁺ In ³⁺	CdSe/Al CdSe/In	UV-visible, PL, FTIR, NMR, ICP-MS, chemical etching	²⁰
Cu _{2-x} Se	Cd ²⁺	CdSe/Cd	UV-visible, PL, SEM, TEM, XRD	²¹
Cu ₂ SeS	Zn ²⁺ , Sn ⁴⁺	Cu ₂ ZnSnSeS	UV-visible, PL, TEM, STEM, XRD, XPS, CV	²²
ZnSe	Cd ²⁺	Zn _{1-x} Cd _x Se	UV-visible, PL, XRD, TEM, STEM-HAADF	²³
ZnSe	Cd ²⁺	Zn _{1-x} Cd _x Se	UV-visible, PL, TEM, XRD, ICP	²⁴
ZnTe	Cd ²⁺	(Zn,Cd)Te	UV-visible, PL, TEM, EDS, STEM-HAADF, PL microscopy	²⁵
PbSe ZnSe ZnSe	Cd ²⁺ Cd ²⁺ Pb ²⁺	CdSe CdSe PbSe	TEM, electron diffraction, RAMAN, EDS	²⁶

ZnS	Tb ³⁺ Eu ³⁺	ZnS/Tb ZnS/Eu	UV-visible, PL	²⁷
ZnS	Tb ³⁺	ZnS/Tb	UV-visible, PL	²⁸
CdSe	Zn ²⁺	Zn _x Cd _{1-x} Se	UV-visible, PL, TEM, XRD	²⁹
CdSe	Zn ²⁺	Zn _x Cd _{1-x} Se	UV-visible, PL, TEM	³⁰
PbSe	Cd ²⁺	PbSe/CdSe	UV-visible, PL, TEM, HAADF-STEM	³¹

^a XRD: X-ray diffraction, XPS: X-ray photoelectron spectroscopy, XANES: X-ray absorption near edge structure, EXAFS: Extended X-ray absorption fine structure spectroscopy, EDS: Energy dispersive X-ray spectroscopy, ICP-MS: Inductively coupled plasma mass spectrometry, ICP-AES: Inductively coupled plasma atomic emission spectroscopy, TEM: Transmission electron microscopy, EFTEM: Energy filtered transmission electron microscopy, SEM: Scanning electron microscopy, STM: Scanning tunnelling microscopy, HAADF-STEM: High angle angular dark-field scanning transmission electron microscopy, UV-Visible: Electronic spectroscopy in ultraviolet-visible spectral range, UV-Vis-NIR: Electronic spectroscopy in ultraviolet-visible-near infrared spectral range, PL: Photoluminescence spectroscopy, EPR: Electron paramagnetic resonance, NMR: Nuclear magnetic resonance, VASP: Vienna Ab initio simulation, FFT: Fast Fourier transform, FTIR: Fourier transform infrared spectroscopy, CV: Cyclic voltammetry.

A. ZnS/M and Zn(Tb)S/M [M = Pb, Hg, Cd, Ca, Mg, Na, K] NPs

Table S2. Elemental Composition of the Nanoparticles Investigated.

System	Zn			S				
ZnS	41.70 ± 0.40			58.30 ± 0.80				
	$[\text{ZnS}]:[\text{M}^{\text{n}+}] = 1:10^{-2}$			$[\text{ZnS}]:[\text{M}^{\text{n}+}] = 1:1$				
ZnS/M	Zn	S	M ⁿ⁺	Zn	S	M ⁿ⁺		
ZnS/Pb	38.18 ± 0.52	60.60 ± 0.25	1.22 ± 0.27	----	50.74 ± 1.79	49.26 ± 1.81		
ZnS/Hg	38.66 ± 1.33	59.74 ± 1.21	1.60 ± 0.13	----	55.93 ± 3.78	44.07 ± 2.71		
ZnS/Cd	41.00 ± 1.14	57.43 ± 1.48	1.57 ± 0.44	17.48 ± 0.55	59.48 ± 1.28	23.04 ± 1.83		
ZnS/Ca	34.41 ± 1.62	65.26 ± 1.55	0.33 ± 0.07	40.20 ± 0.73	59.05 ± 0.67	0.75 ± 0.05		
ZnS/Mg	41.57 ± 1.88	57.18 ± 2.21	1.25 ± 0.32	41.57 ± 1.38	57.32 ± 1.44	1.11 ± 0.06		
ZnS/Na	45.32 ± 1.83	54.48 ± 1.87	0.20 ± 0.04	40.25 ± 1.14	59.41 ± 1.10	0.34 ± 0.04		
ZnS/K	45.66 ± 5.81	54.13 ± 5.80	0.21 ± 0.02	41.39 ± 1.64	58.29 ± 1.60	0.32 ± 0.04		
System	Zn		Tb		S			
Zn(Tb)S	39.40 ± 0.50		5.8 ± 0.42		54.80 ± 0.60			
	$[\text{Zn(Tb)S}]:[\text{M}^{\text{n}+}] = 1:10^{-2}$			$[\text{Zn(Tb)S}]:[\text{M}^{\text{n}+}] = 1:1$				
Zn(Tb)S/M	Zn	Tb	S	M ⁿ⁺	Zn	Tb	S	M ⁿ⁺
Zn(Tb)S/Pb	33.16 ± 3.54	5.63 ± 0.25	59.55 ± 3.58	1.66 ± 0.21	----	1.19 ± 0.17	51.77 ± 0.21	47.04 ± 0.38
Zn(Tb)S/Hg	38.35 ± 3.98	3.47 ± 0.33	56.30 ± 3.44	1.88 ± 0.86	----	1.23 ± 0.37	53.46 ± 2.18	45.31 ± 1.81
Zn(Tb)S/Cd	32.76 ± 0.98	4.96 ± 0.50	60.64 ± 0.48	1.64 ± 0.01	14.39 ± 0.12	4.90 ± 0.30	56.36 ± 1.11	24.35 ± 0.64
Zn(Tb)S/Ca	32.67 ± 1.03	3.22 ± 0.16	63.46 ± 1.10	0.65 ± 0.20	36.28 ± 3.07	4.25 ± 0.15	57.92 ± 3.55	1.55 ± 0.62
Zn(Tb)S/Mg	36.66 ± 1.37	3.29 ± 0.40	59.30 ± 1.57	0.75 ± 0.21	36.72 ± 2.60	3.36 ± 0.31	58.26 ± 2.62	1.66 ± 0.33
Zn(Tb)S/Na	37.06 ± 1.80	4.07 ± 0.83	58.63 ± 1.05	0.24 ± 0.08	36.42 ± 0.15	4.73 ± 0.13	57.21 ± 1.49	1.64 ± 0.21
Zn(Tb)S/K	37.69 ± 3.74	3.91 ± 0.64	58.14 ± 3.17	0.26 ± 0.06	36.91 ± 0.86	4.68 ± 0.49	56.88 ± 1.53	1.53 ± 0.18

Thermodynamic Consideration. A calculation based on thermodynamic consideration can predict the feasibility of cation exchange reaction.³² For a reaction between MN and P⁺ producing PN and Mⁿ⁺ a lower solubility product constant of PN and higher standard reduction potential of a P^{n+/P} redox pair confer a feasible cation exchange reaction. The standard free energy of reaction ($\Delta G^0_{\text{reaction}}$) can be computed by equation (1)

$$\Delta G_{\text{reaction}}^0 = \Delta_f G^0 (\text{PN}) - \Delta_f G^0 (\text{MN}) - 2F[E_0(\text{P}^{n+}/\text{P}) - E_0(\text{M}^{n+}/\text{M})] \quad (1)$$

where F is the Faraday's constant.

The parameters obtained from this analysis are presented in Table S3. $\Delta G_{\text{reaction}}^0$ for Zn^{2+} – M^{n+} exchange pairs for sulfides decreases in the order $\text{Hg}^{2+} < \text{Cd}^{2+} < \text{Pb}^{2+} < \text{Ca}^{2+} < \text{Mg}^{2+} < \text{K}^+ < \text{Na}^+$. Most importantly; for Hg^{2+} , Pb^{2+} , and Cd^{2+} this value is negative, pointing to a favorable cation exchange reaction. For the other four cations investigated a positive ΔG value suggests an unfavorable exchange interaction.

Table S3. A Summary of Thermodynamic Parameters for the Cation Pairs Studied.

System	Standard Free Energy of Formation $\Delta_f G^0$ (kJmol ⁻¹)	System (M^{n+})	Standard Reduction Potential (E_0) (V) (M^{n+}/M)	Reactant → Product	$\Delta G_{\text{reaction}}^0$ (kJmol ⁻¹)
ZnS	-201.3	Zn ²⁺ /Zn	-0.762		
PbS	-98.7	Pb ²⁺ /Pb	-0.126	ZnS → PbS	-20.2
HgS	-50.6	Hg ²⁺ /Hg	+0.852	ZnS → HgS	-160.8
CdS	-156.5	Cd ²⁺ /Cd	-0.402	ZnS → CdS	-24.7
CaS	-477.4	Ca ²⁺ /Ca	-2.868	ZnS → CaS	+130.4
MgS	-341.8	Mg ²⁺ /Mg	-2.360	ZnS → MgS	+167.9
Na ₂ S	-354.8	Na ⁺ /Na	-2.714	ZnS → Na₂S	+223.2
K ₂ S	-404.2	K ⁺ /K	-2.936	ZnS → K₂S	+216.7

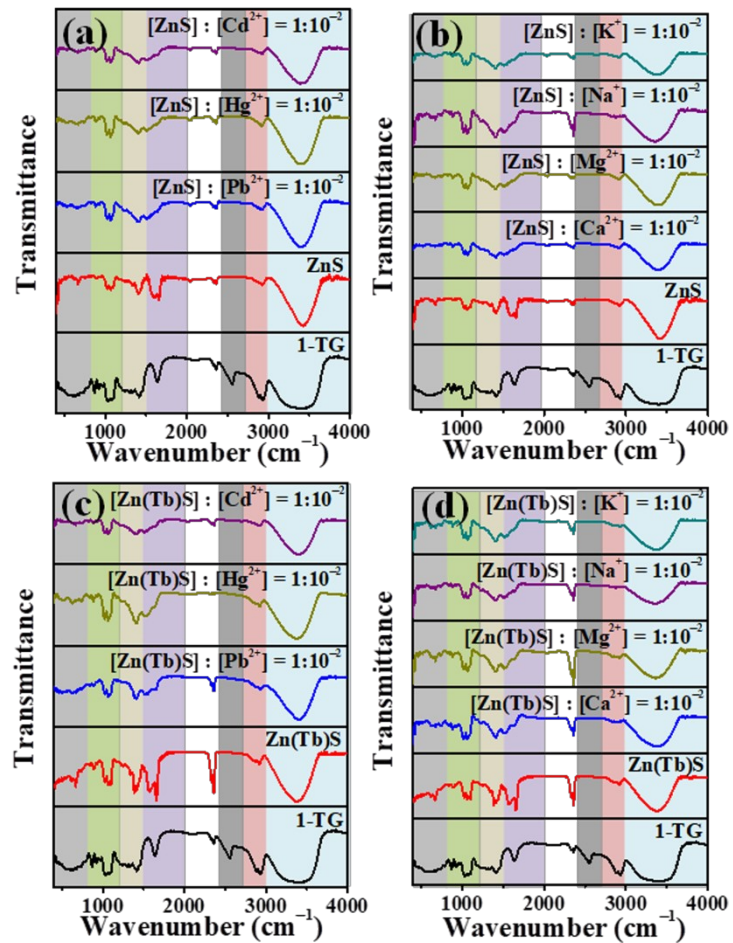


Figure S1. FTIR spectra of (a) $[ZnS] : [M^{n+}] = 1:10^{-2}$ ($M^{n+} = Pb^{2+}, Hg^{2+}, Cd^{2+}$), (b) $[ZnS] : [M^{n+}] = 1:10^{-2}$ ($M^{n+} = Ca^{2+}, Mg^{2+}, Na^+, K^+$), (c) $[Zn(Tb)S] : [M^{n+}] = 1:10^{-2}$ ($M^{n+} = Pb^{2+}, Hg^{2+}, Cd^{2+}$), (d) $[Zn(Tb)S] : [M^{n+}] = 1:10^{-2}$ ($M^{n+} = Ca^{2+}, Mg^{2+}, Na^+, K^+$) are shown.

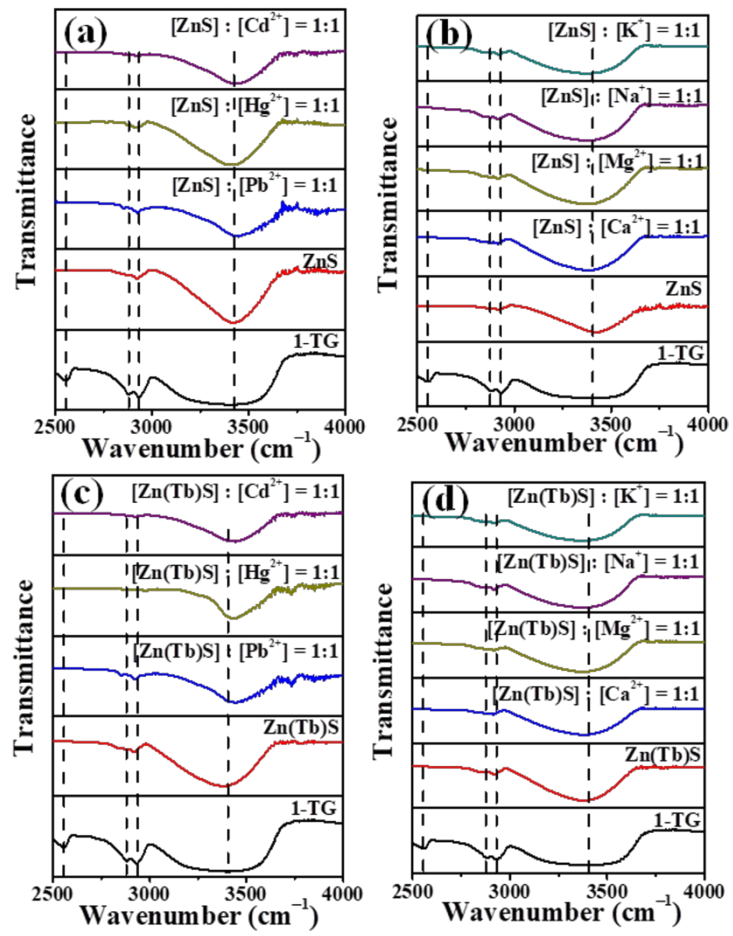


Figure S2. FTIR spectra ($2500\text{-}4000\text{ cm}^{-1}$) of (a) $[\text{ZnS}] : [\text{M}^{\text{n}+}] = 1:1$ ($\text{M}^{\text{n}+} = \text{Pb}^{2+}, \text{Hg}^{2+}, \text{Cd}^{2+}$), (b) $[\text{ZnS}] : [\text{M}^{\text{n}+}] = 1:1$ ($\text{M}^{\text{n}+} = \text{Ca}^{2+}, \text{Mg}^{2+}, \text{Na}^+, \text{K}^+$), (c) $[\text{Zn}(\text{Tb})\text{S}] : [\text{M}^{\text{n}+}] = 1:1$ ($\text{M}^{\text{n}+} = \text{Pb}^{2+}, \text{Hg}^{2+}, \text{Cd}^{2+}$), (d) $[\text{Zn}(\text{Tb})\text{S}] : [\text{M}^{\text{n}+}] = 1:1$ ($\text{M}^{\text{n}+} = \text{Ca}^{2+}, \text{Mg}^{2+}, \text{Na}^+, \text{K}^+$) are shown.

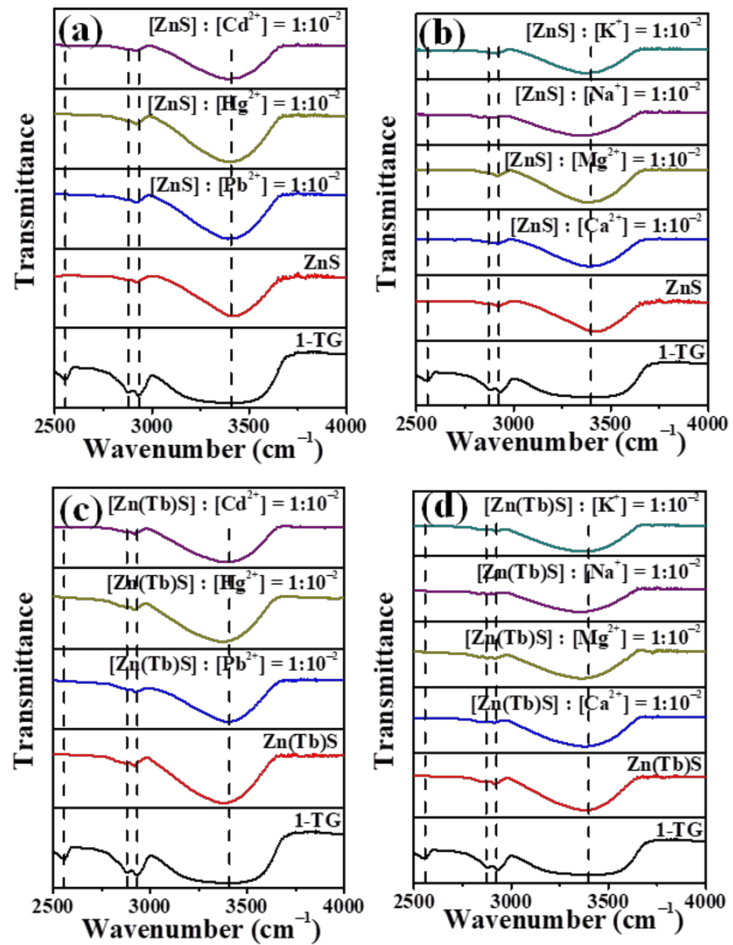


Figure S3. FTIR spectra ($2500\text{-}4000\text{ cm}^{-1}$) of (a) $[\text{ZnS}] : [\text{M}^{\text{n}+}] = 1:10^{-2}$ ($\text{M}^{\text{n}+} = \text{Pb}^{2+}, \text{Hg}^{2+}, \text{Cd}^{2+}$), (b) $[\text{ZnS}] : [\text{M}^{\text{n}+}] = 1:10^{-2}$ ($\text{M}^{\text{n}+} = \text{Ca}^{2+}, \text{Mg}^{2+}, \text{Na}^+, \text{K}^+$), (c) $[\text{Zn}(\text{Tb})\text{S}] : [\text{M}^{\text{n}+}] = 1:10^{-2}$ ($\text{M}^{\text{n}+} = \text{Pb}^{2+}, \text{Hg}^{2+}, \text{Cd}^{2+}$), (d) $[\text{Zn}(\text{Tb})\text{S}] : [\text{M}^{\text{n}+}] = 1:10^{-2}$ ($\text{M}^{\text{n}+} = \text{Ca}^{2+}, \text{Mg}^{2+}, \text{Na}^+, \text{K}^+$) are shown.

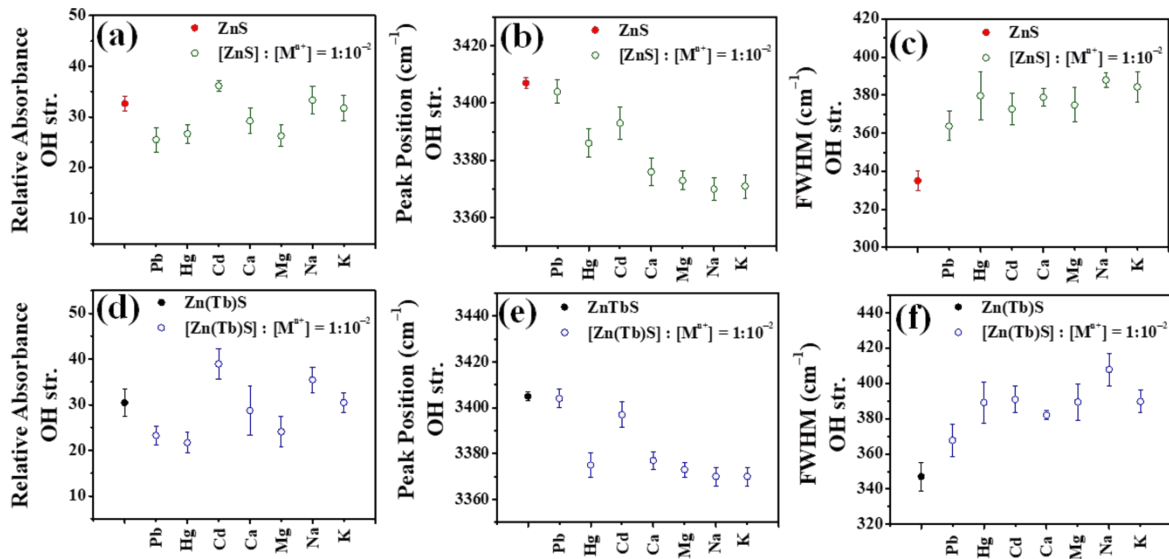


Figure S4. Spectral parameters of OH stretching band (a) relative absorption, (b) peak position, (c) FWHM of $[ZnS] : [M^{n+}] = 1:10^{-2}$ and $[Zn(Tb)S] : [M^{n+}] = 1:10^{-2}$ are shown in panels (a) – (c) and (d) – (f), respectively.

Table S4. Spectral Parameters of OH Stretching Absorption Band of $[ZnS] : [M^{n+}] = 1:10^{-2}$ and 1:1 and $[Zn(Tb)S] : [M^{n+}] = 1:10^{-2}$ and 1:1.

System	Relative absorbance $\int [I_{OH\ str.}]dv / \int [I_{CH2\ str.}]dv$		Spectral peak position (cm^{-1})		FWHM (cm^{-1})	
1-TG	7.53 ± 0.14		3400 ± 1		455 ± 20	
ZnS	32.65 ± 1.51		3407 ± 2		335 ± 5	
ZnS/M	$1:10^{-2}$	1:1	$1:10^{-2}$	1:1	$1:10^{-2}$	1:1
ZnS/Pb	25.53 ± 2.44	11.47 ± 2.82	3404 ± 4	3436 ± 6	364 ± 8	354 ± 13
ZnS/Hg	26.67 ± 1.79	13.65 ± 2.35	3386 ± 5	3422 ± 6	380 ± 12	348 ± 18
ZnS/Cd	36.12 ± 1.10	31.94 ± 6.05	3393 ± 6	3426 ± 4	373 ± 8	368 ± 3
ZnS/Ca	29.22 ± 2.52	26.29 ± 2.90	3376 ± 5	3375 ± 11	379 ± 5	389 ± 9
ZnS/Mg	26.28 ± 2.11	33.66 ± 2.54	3373 ± 3	3373 ± 8	375 ± 9	397 ± 3
ZnS/Na	33.28 ± 2.75	35.79 ± 6.04	3370 ± 4	3377 ± 3	388 ± 4	379 ± 5
ZnS/K	31.74 ± 2.53	26.34 ± 2.75	3371 ± 4	3377 ± 3	384 ± 8	375 ± 3
Zn(Tb)S	30.44 ± 3.04		3405 ± 2		347 ± 8	
Zn(Tb)S/M	$1:10^{-2}$	1:1	$1:10^{-2}$	1:1	$1:10^{-2}$	1:1
Zn(Tb)S/Pb	23.24 ± 2.11	12.43 ± 2.46	3404 ± 4	3440 ± 5	368 ± 9	358 ± 24
Zn(Tb)S/Hg	21.69 ± 2.19	14.41 ± 1.48	3375 ± 6	3432 ± 4	389 ± 12	323 ± 18
Zn(Tb)S/Cd	38.94 ± 3.34	28.60 ± 3.08	3397 ± 6	3433 ± 4	391 ± 7	385 ± 10
Zn(Tb)S/Ca	28.69 ± 5.36	33.36 ± 1.96	3377 ± 4	3375 ± 12	382 ± 2	404 ± 4
Zn(Tb)S/Mg	24.06 ± 3.39	36.56 ± 5.49	3373 ± 3	3374 ± 9	389 ± 10	407 ± 7
Zn(Tb)S/Na	35.43 ± 2.75	28.08 ± 2.26	3370 ± 4	3377 ± 3	408 ± 9	391 ± 8
Zn(Tb)S/K	30.47 ± 2.14	26.32 ± 1.11	3370 ± 4	3377 ± 3	390 ± 7	389 ± 7

Table S5. Comparison of Methylene Stretching IR Absorption Band Spectral Properties in the Different Systems Investigated.

System	$I[v_{as}[\text{CH}_2]] / I[v_s[\text{CH}_2]]$		$\int I[v_{as}[\text{CH}_2]] dv / \int I[v_s[\text{CH}_2]] dv$		FWHM $[v_{as}[\text{CH}_2]]$ (cm $^{-1}$)		FWHM $[v_s[\text{CH}_2]]$ (cm $^{-1}$)	
1-TG	2.23 ± 0.11		2.76 ± 0.11		46 ± 4		30 ± 1	
ZnS	5.40 ± 0.05		5.00 ± 0.47		47 ± 5		38 ± 6	
ZnS/M	$1:10^{-2}$	1:1	$1:10^{-2}$	1:1	$1:10^{-2}$	1:1	$1:10^{-2}$	1:1
ZnS/Pb	3.02 ± 0.03	2.75 ± 0.32	3.00 ± 0.21	2.60 ± 0.68	38 ± 5	33 ± 2	25 ± 2	21 ± 1
ZnS/Hg	3.35 ± 0.35	2.47 ± 0.13	2.41 ± 0.30	1.98 ± 0.14	37 ± 4	37 ± 5	27 ± 1	26 ± 5
ZnS/Cd	5.33 ± 0.40	2.78 ± 0.30	2.95 ± 0.10	2.91 ± 0.86	48 ± 2	44 ± 1	27 ± 1	27 ± 2
ZnS/Ca	3.53 ± 0.52	3.15 ± 0.50	2.65 ± 0.29	2.29 ± 0.23	49 ± 5	44 ± 4	28 ± 2	26 ± 1
ZnS/Mg	3.40 ± 0.35	3.30 ± 0.56	3.02 ± 0.15	2.51 ± 0.18	45 ± 4	47 ± 3	27 ± 1	27 ± 3
ZnS/Na	5.16 ± 0.37	4.02 ± 0.06	2.83 ± 0.14	2.95 ± 0.14	46 ± 6	45 ± 4	29 ± 3	26 ± 2
ZnS/K	4.84 ± 0.11	3.46 ± 0.47	2.71 ± 0.76	2.04 ± 0.17	47 ± 1	44 ± 6	28 ± 3	26 ± 3
Zn(Tb)S	5.35 ± 1.12		6.22 ± 1.22		35 ± 1		26 ± 4	
Zn(Tb)S/M	$1:10^{-2}$	1:1	$1:10^{-2}$	1:1	$1:10^{-2}$	1:1	$1:10^{-2}$	1:1
Zn(Tb)S/Pb	3.10 ± 0.57	3.00 ± 0.42	2.15 ± 0.76	2.76 ± 0.57	41 ± 1	33 ± 2	29 ± 3	22 ± 3
Zn(Tb)S/Hg	2.63 ± 0.66	2.12 ± 0.45	2.76 ± 0.47	1.45 ± 0.50	43 ± 2	36 ± 5	21 ± 4	25 ± 7
Zn(Tb)S/Cd	4.50 ± 1.56	2.25 ± 1.20	2.95 ± 0.64	4.10 ± 0.60	37 ± 1	31 ± 4	29 ± 4	21 ± 4
Zn(Tb)S/Ca	2.85 ± 0.35	2.86 ± 0.51	1.91 ± 0.33	2.29 ± 0.23	38 ± 2	29 ± 1	22 ± 4	25 ± 5
Zn(Tb)S/Mg	2.97 ± 0.89	3.18 ± 0.92	2.23 ± 0.94	2.52 ± 0.50	38 ± 6	31 ± 4	22 ± 3	21 ± 1
Zn(Tb)S/Na	4.45 ± 1.20	4.20 ± 1.26	3.75 ± 0.80	3.06 ± 0.01	34 ± 4	34 ± 3	25 ± 4	22 ± 1
Zn(Tb)S/K	3.50 ± 0.85	3.95 ± 0.78	3.64 ± 0.81	1.65 ± 0.01	35 ± 4	36 ± 1	22 ± 2	30 ± 1

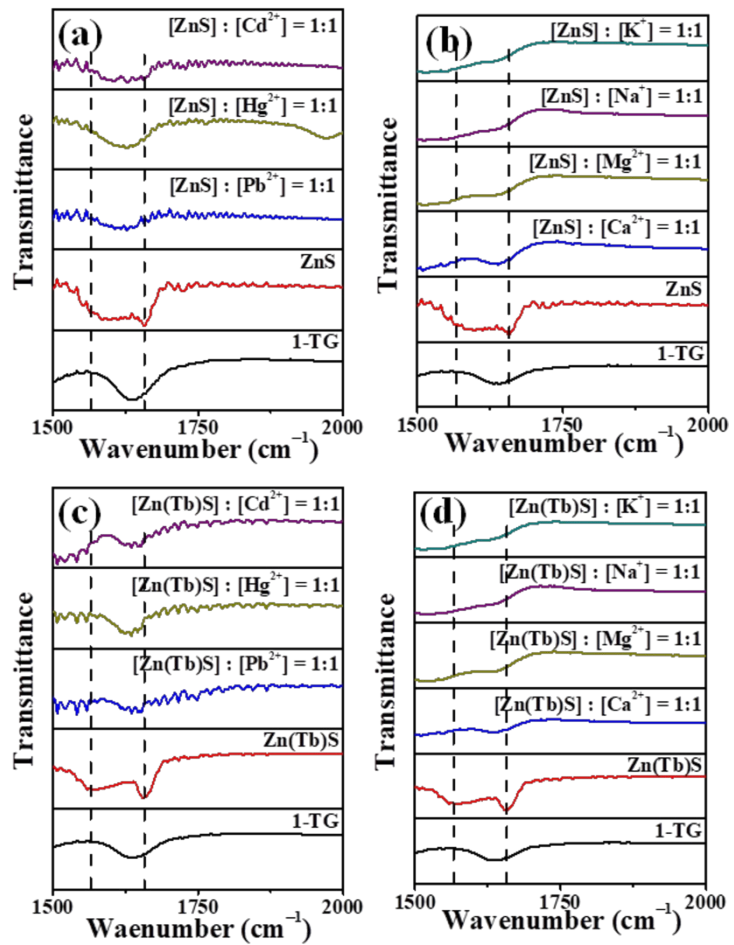


Figure S5. FTIR spectra ($1500\text{-}2000\text{ cm}^{-1}$) of (a) $[\text{ZnS}] : [\text{M}^{\text{n}+}] = 1:1$ ($\text{M}^{\text{n}+} = \text{Pb}^{2+}, \text{Hg}^{2+}, \text{Cd}^{2+}$), (b) $[\text{ZnS}] : [\text{M}^{\text{n}+}] = 1:1$ ($\text{M}^{\text{n}+} = \text{Ca}^{2+}, \text{Mg}^{2+}, \text{Na}^+, \text{K}^+$), (c) $[\text{Zn}(\text{Tb})\text{S}] : [\text{M}^{\text{n}+}] = 1:1$ ($\text{M}^{\text{n}+} = \text{Pb}^{2+}, \text{Hg}^{2+}, \text{Cd}^{2+}$), (d) $[\text{Zn}(\text{Tb})\text{S}] : [\text{M}^{\text{n}+}] = 1:1$ ($\text{M}^{\text{n}+} = \text{Ca}^{2+}, \text{Mg}^{2+}, \text{Na}^+, \text{K}^+$) are shown.

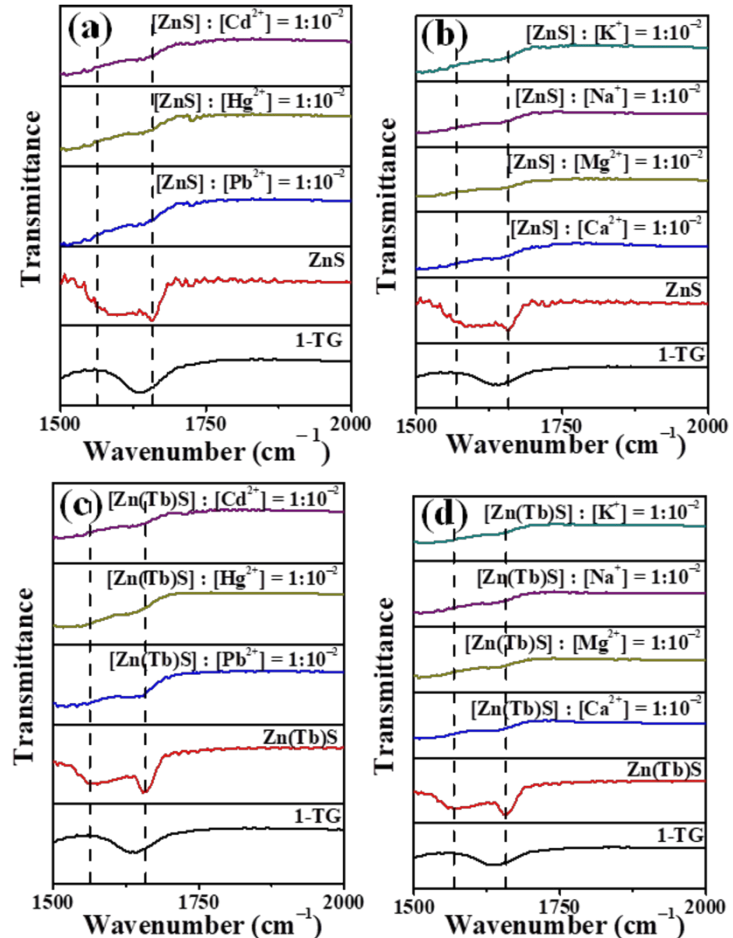


Figure S6. FTIR spectra ($1500\text{-}2000 \text{ cm}^{-1}$) of (a) $[\text{ZnS}] : [\text{M}^{\text{n}+}] = 1:10^{-2}$ ($\text{M}^{\text{n}+} = \text{Pb}^{2+}, \text{Hg}^{2+}, \text{Cd}^{2+}$), (b) $[\text{ZnS}] : [\text{M}^{\text{n}+}] = 1:10^{-2}$ ($\text{M}^{\text{n}+} = \text{Ca}^{2+}, \text{Mg}^{2+}, \text{Na}^+, \text{K}^+$), (c) $[\text{Zn(Tb)S}] : [\text{M}^{\text{n}+}] = 1:10^{-2}$ ($\text{M}^{\text{n}+} = \text{Pb}^{2+}, \text{Hg}^{2+}, \text{Cd}^{2+}$), (d) $[\text{Zn(Tb)S}] : [\text{M}^{\text{n}+}] = 1:10^{-2}$ ($\text{M}^{\text{n}+} = \text{Ca}^{2+}, \text{Mg}^{2+}, \text{Na}^+, \text{K}^+$) are shown.

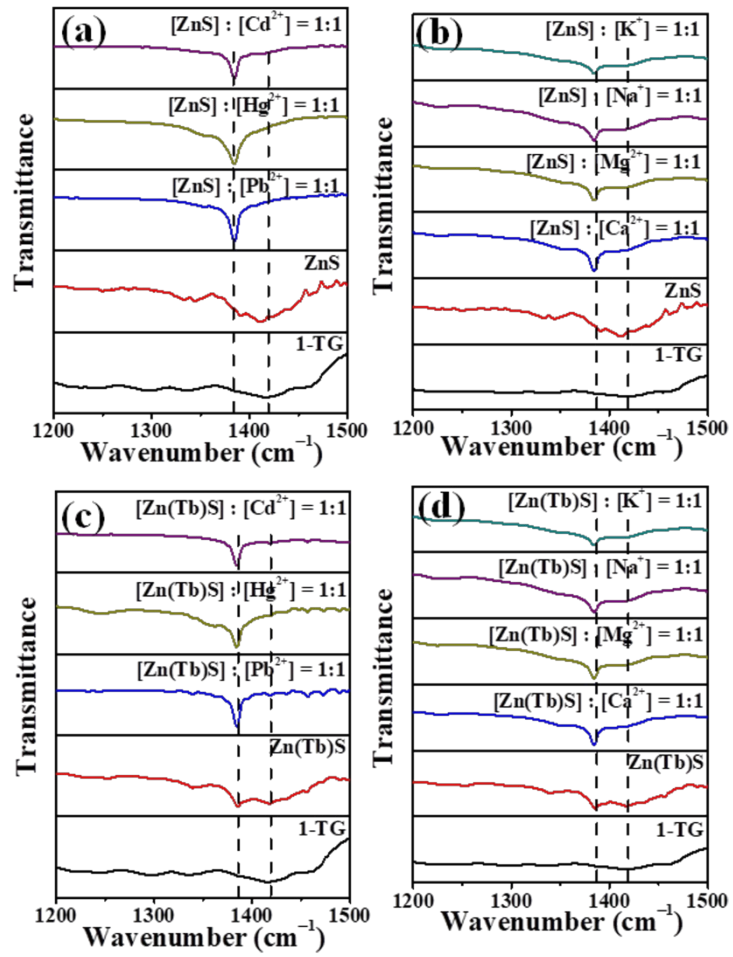


Figure S7. FTIR spectra ($1200\text{-}1500 \text{ cm}^{-1}$) of (a) $[\text{ZnS}] : [\text{Mn}^+] = 1:1$ ($\text{Mn}^+ = \text{Pb}^{2+}, \text{Hg}^{2+}, \text{Cd}^{2+}$), (b) $[\text{ZnS}] : [\text{Mn}^+] = 1:1$ ($\text{Mn}^+ = \text{Ca}^{2+}, \text{Mg}^{2+}, \text{Na}^+, \text{K}^+$), (c) $[\text{Zn}(\text{Tb})\text{S}] : [\text{Mn}^+] = 1:1$ ($\text{Mn}^+ = \text{Pb}^{2+}, \text{Hg}^{2+}, \text{Cd}^{2+}$), (d) $[\text{Zn}(\text{Tb})\text{S}] : [\text{Mn}^+] = 1:1$ ($\text{Mn}^+ = \text{Ca}^{2+}, \text{Mg}^{2+}, \text{Na}^+, \text{K}^+$) are shown.

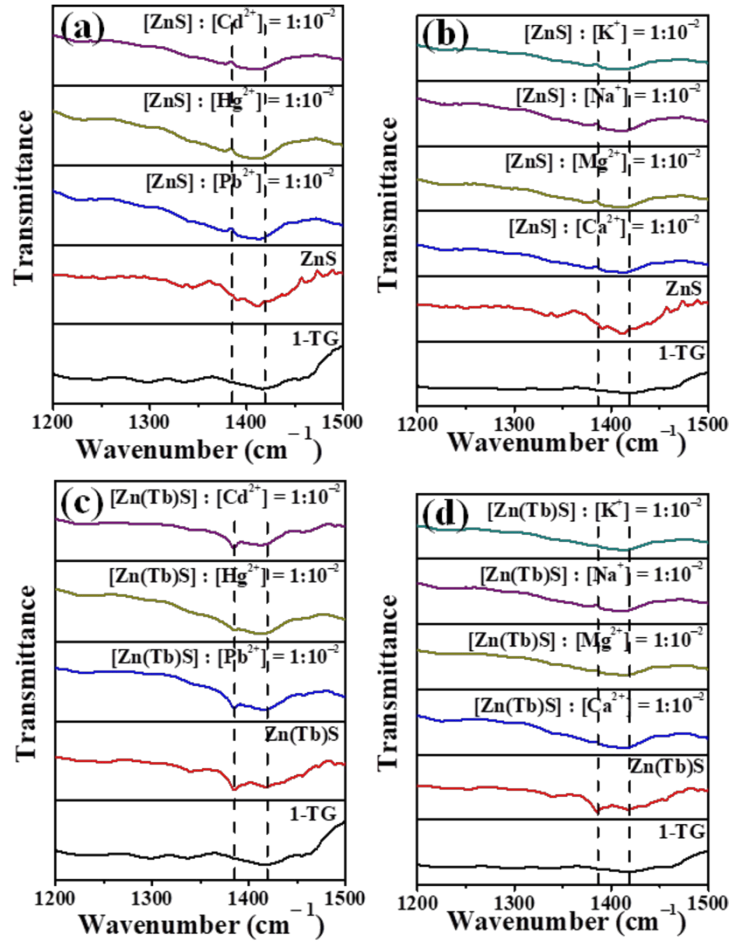


Figure S8. FTIR spectra (1200-1500 cm⁻¹) of (a) [ZnS] : [Mⁿ⁺] = 1:10⁻² (Mⁿ⁺ = Pb²⁺, Hg²⁺, Cd²⁺), (b) [ZnS] : [Mⁿ⁺] = 1: 10⁻² (Mⁿ⁺ = Ca²⁺, Mg²⁺, Na⁺, K⁺), (c) [Zn(Tb)S] : [Mⁿ⁺] = 1: 10⁻² (Mⁿ⁺ = Pb²⁺, Hg²⁺, Cd²⁺), (d) [Zn(Tb)S] : [Mⁿ⁺] = 1: 10⁻² (Mⁿ⁺ = Ca²⁺, Mg²⁺, Na⁺, K⁺) are shown.

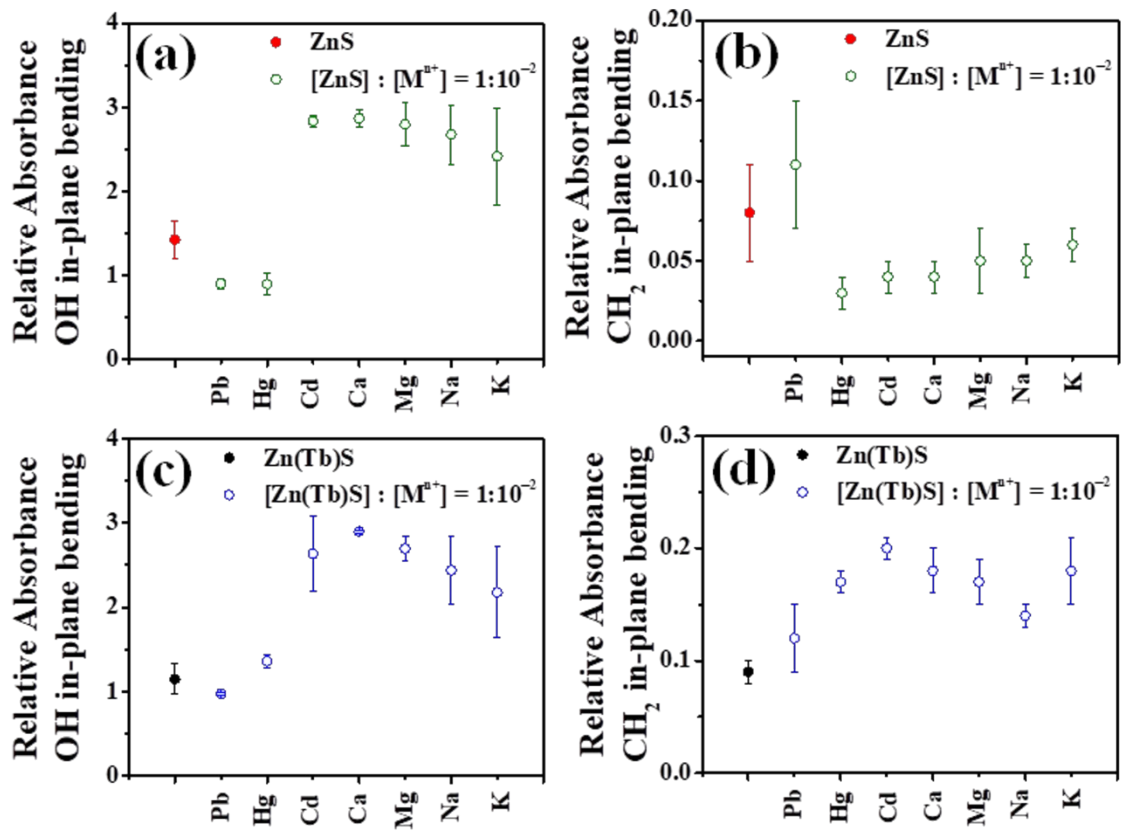


Figure S9. Trend in relative absorption of OH and CH_2 in-plane bending vibrations in $[ZnS] : [M^{n+}] = 1:10^{-2}$ and $[Zn(Tb)S] : [M^{n+}] = 1:10^{-2}$ are shown in panels (a) – (b) and (c) – (d), respectively.

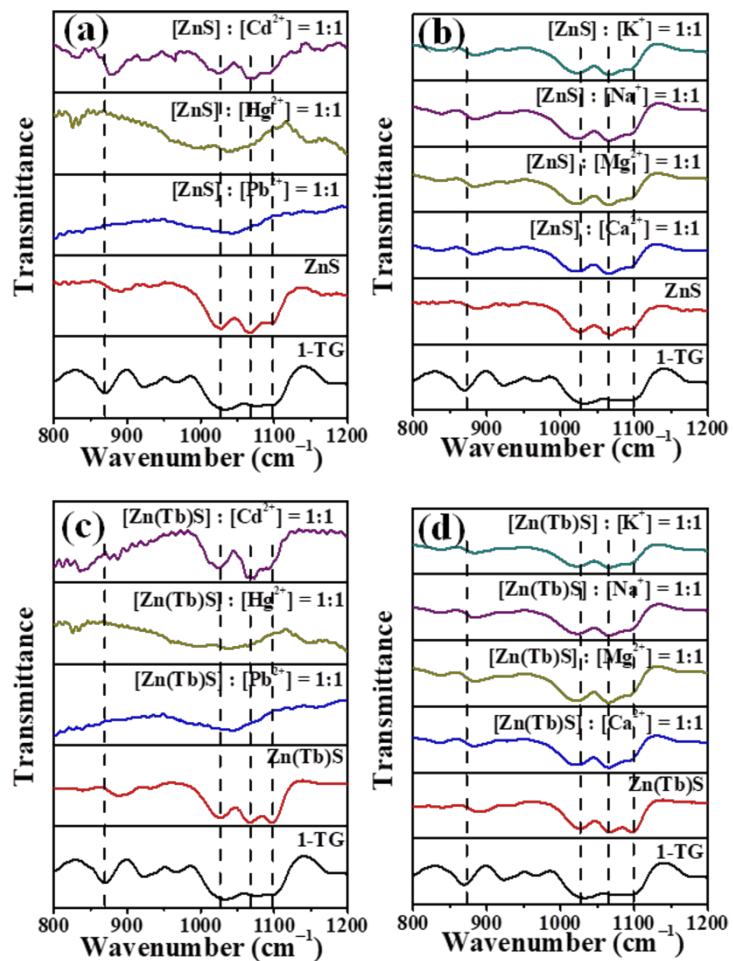


Figure S10. FTIR spectra ($800\text{-}1200\text{ cm}^{-1}$) of (a) $[\text{ZnS}] : [\text{M}^{\text{n}+}] = 1:1$ ($\text{M}^{\text{n}+} = \text{Pb}^{2+}, \text{Hg}^{2+}, \text{Cd}^{2+}$), (b) $[\text{ZnS}] : [\text{M}^{\text{n}+}] = 1:1$ ($\text{M}^{\text{n}+} = \text{Ca}^{2+}, \text{Mg}^{2+}, \text{Na}^+, \text{K}^+$), (c) $[\text{Zn}(\text{Tb})\text{S}] : [\text{M}^{\text{n}+}] = 1:1$ ($\text{M}^{\text{n}+} = \text{Pb}^{2+}, \text{Hg}^{2+}, \text{Cd}^{2+}$), (d) $[\text{Zn}(\text{Tb})\text{S}] : [\text{M}^{\text{n}+}] = 1:1$ ($\text{M}^{\text{n}+} = \text{Ca}^{2+}, \text{Mg}^{2+}, \text{Na}^+, \text{K}^+$) are shown.

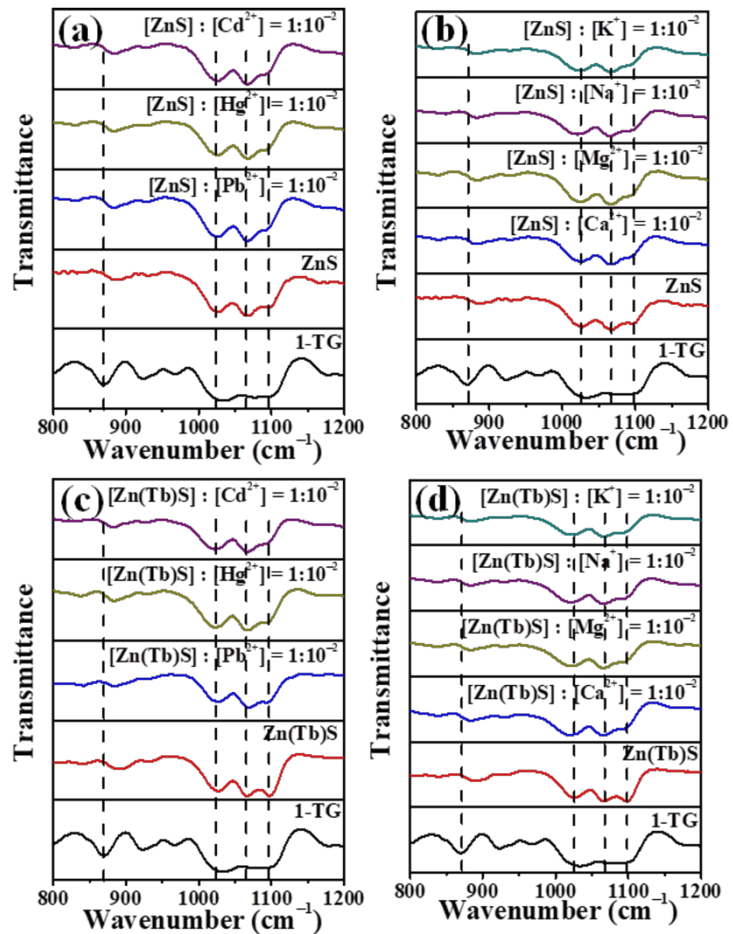


Figure S11. FTIR spectra (800-1200 cm⁻¹) of (a) [ZnS] : [Mⁿ⁺] = 1:10⁻² (Mⁿ⁺ = Pb²⁺, Hg²⁺, Cd²⁺), (b) [ZnS] : [Mⁿ⁺] = 1:10⁻² (Mⁿ⁺ = Ca²⁺, Mg²⁺, Na⁺, K⁺), (c) [Zn(Tb)S] : [Mⁿ⁺] = 1:10⁻² (Mⁿ⁺ = Pb²⁺, Hg²⁺, Cd²⁺), (d) [Zn(Tb)S] : [Mⁿ⁺] = 1:10⁻² (Mⁿ⁺ = Ca²⁺, Mg²⁺, Na⁺, K⁺) are shown.

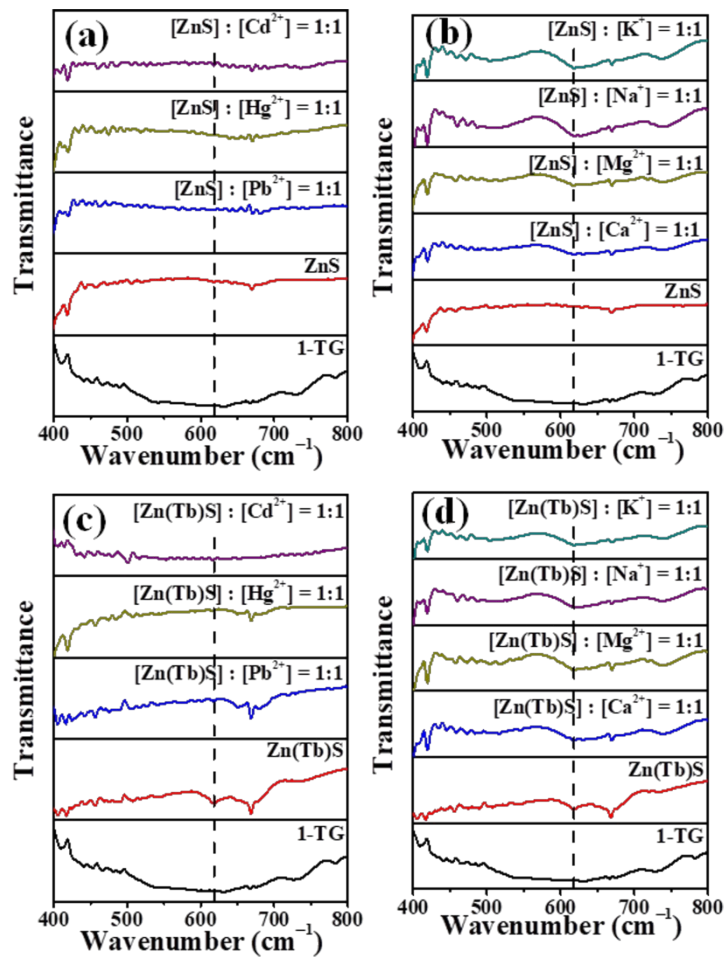


Figure S12. FTIR spectra ($400\text{-}800\text{ cm}^{-1}$) of (a) $[\text{ZnS}] : [\text{M}^{\text{n}+}] = 1:1$ ($\text{M}^{\text{n}+} = \text{Pb}^{2+}, \text{Hg}^{2+}, \text{Cd}^{2+}$), (b) $[\text{ZnS}] : [\text{M}^{\text{n}+}] = 1:1$ ($\text{M}^{\text{n}+} = \text{Ca}^{2+}, \text{Mg}^{2+}, \text{Na}^+, \text{K}^+$), (c) $[\text{Zn}(\text{Tb})\text{S}] : [\text{M}^{\text{n}+}] = 1:1$ ($\text{M}^{\text{n}+} = \text{Pb}^{2+}, \text{Hg}^{2+}, \text{Cd}^{2+}$), (d) $[\text{Zn}(\text{Tb})\text{S}] : [\text{M}^{\text{n}+}] = 1:1$ ($\text{M}^{\text{n}+} = \text{Ca}^{2+}, \text{Mg}^{2+}, \text{Na}^+, \text{K}^+$) are shown.

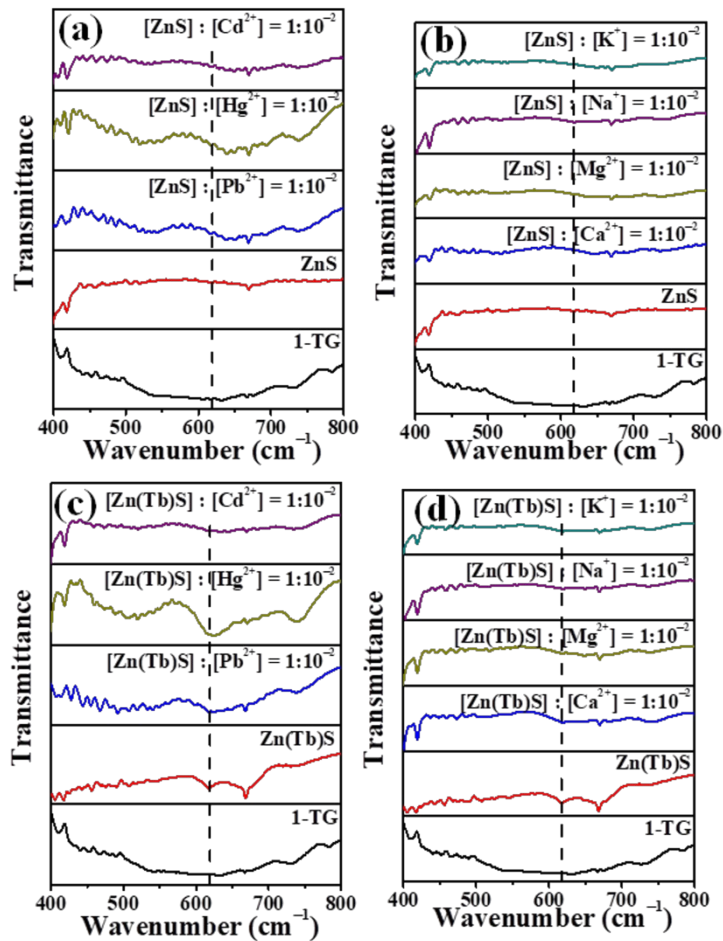


Figure S13. FTIR spectra (400-800 cm⁻¹) of (a) [ZnS] : [Mⁿ⁺] = 1:10⁻² (Mⁿ⁺ = Pb²⁺, Hg²⁺, Cd²⁺), (b) [ZnS] : [Mⁿ⁺] = 1:10⁻² (Mⁿ⁺ = Ca²⁺, Mg²⁺, Na⁺, K⁺), (c) [Zn(Tb)S] : [Mⁿ⁺] = 1: 10⁻² (Mⁿ⁺ = Pb²⁺, Hg²⁺, Cd²⁺), (d) [Zn(Tb)S] : [Mⁿ⁺] = 1: 10⁻² (Mⁿ⁺ = Ca²⁺, Mg²⁺, Na⁺, K⁺) are shown.

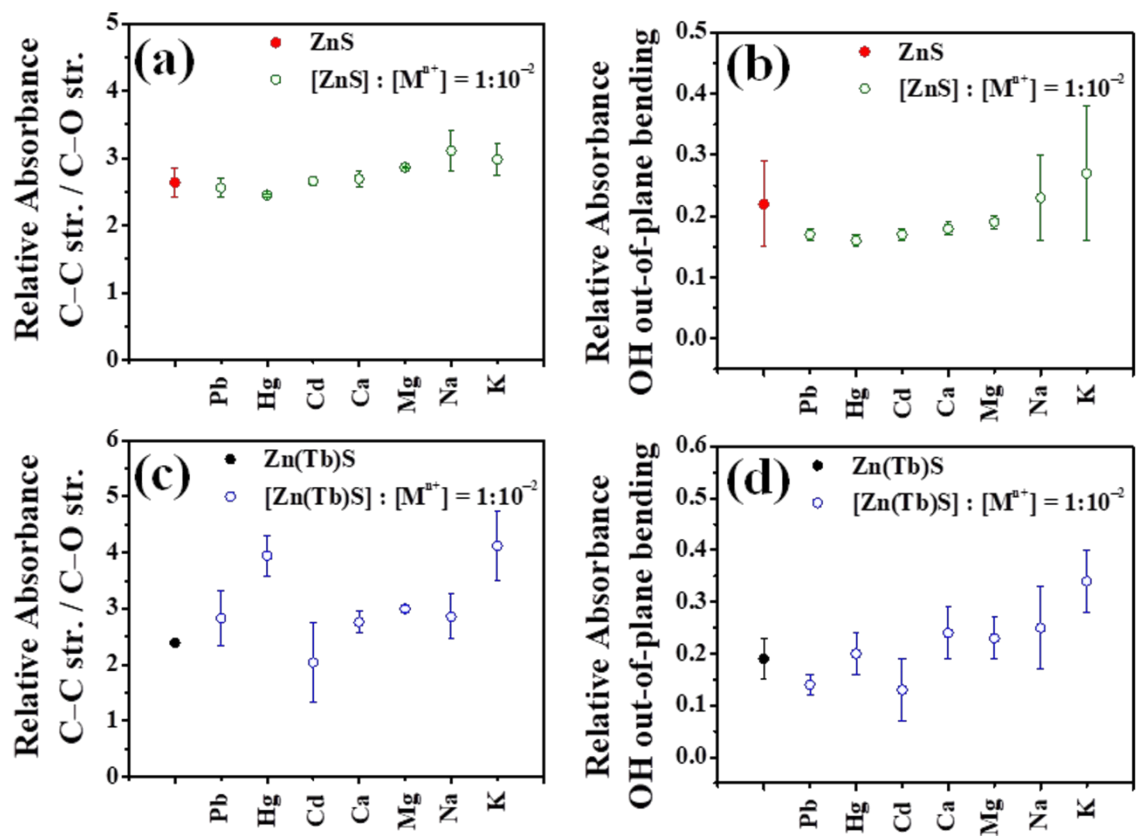


Figure S14. Trend in relative absorption of C–C stretching, C–O stretching, and OH out-of-plane bending vibrations in $[ZnS] : [M^{n+}] = 1:10^{-2}$ and $[Zn(Tb)S] : [M^{n+}] = 1: 10^{-2}$ are shown in panels (a) – (b) and (c) – (d), respectively.

Table S6. Comparison of (a) OH in-plane bending, (b) CH₂ in-plane bending, (c) C–C str. / C–O str., and (d) OH out-of-plane bending IR Absorption Band Spectral Properties in the Different Systems Investigated.

System	Normalize d absorbance $\int [I_{OH \text{ in-plane bending}}] dv / \int [I_{CH_2 \text{ str.}}] dv$		Normalize d absorbance $\int [I_{CH_2 \text{ in-plane bending}}] dv / \int [I_{CH_2 \text{ str.}}] dv$		Normalize d absorbance $\int [I_{\text{C-C str. / C-O str.}}] dv / \int [I_{CH_2 \text{ str.}}] dv$		Normalize d absorbance $\int [I_{OH \text{ out-of-plane bending}}] dv / \int [I_{CH_2 \text{ str.}}] dv$	
1-TG	0.55 ± 0.06		0.16 ± 0.01		0.96 ± 0.16		0.14 ± 0.01	
ZnS	1.43 ± 0.22		0.08 ± 0.03		2.64 ± 0.21		0.22 ± 0.07	
ZnS/M	$1:10^{-2}$	1:1	$1:10^{-2}$	1:1	$1:10^{-2}$	1:1	$1:10^{-2}$	1:1
ZnS/Pb	0.91 ± 0.06	0.27 ± 0.02	0.11 ± 0.04	8.96 ± 0.20	2.56 ± 0.14	1.01 ± 0.30	0.17 ± 0.01	--
ZnS/Hg	0.90 ± 0.13	0.41 ± 0.14	0.03 ± 0.01	8.18 ± 0.90	2.45 ± 0.02	1.19 ± 0.43	0.16 ± 0.01	--
ZnS/Cd	2.84 ± 0.07	1.30 ± 0.28	0.04 ± 0.01	6.58 ± 0.75	2.66 ± 0.06	1.60 ± 0.39	0.17 ± 0.01	0.26 ± 0.04
ZnS/Ca	2.88 ± 0.11	2.70 ± 0.27	0.04 ± 0.01	0.81 ± 0.01	2.69 ± 0.11	2.78 ± 0.03	0.18 ± 0.01	0.29 ± 0.03
ZnS/Mg	2.80 ± 0.25	2.75 ± 0.35	0.05 ± 0.02	0.79 ± 0.02	2.86 ± 0.01	3.40 ± 0.69	0.19 ± 0.01	0.27 ± 0.06
ZnS/Na	2.68 ± 0.35	2.45 ± 0.49	0.05 ± 0.01	0.59 ± 0.04	3.11 ± 0.31	3.19 ± 0.26	0.23 ± 0.07	0.21 ± 0.03
ZnS/K	2.42 ± 0.58	2.55 ± 0.49	0.06 ± 0.01	0.41 ± 0.06	2.98 ± 0.23	3.43 ± 0.11	0.27 ± 0.11	0.18 ± 0.01
Zn(Tb)S	1.15 ± 0.18		0.09 ± 0.01		2.39 ± 0.03		0.19 ± 0.04	
Zn(Tb)S/M	$1:10^{-2}$	1:1	$1:10^{-2}$	1:1	$1:10^{-2}$	1:1	$1:10^{-2}$	1:1
Zn(Tb)S/Pb	0.98 ± 0.02	0.25 ± 0.01	0.12 ± 0.03	7.90 ± 0.66	2.83 ± 0.48	0.72 ± 0.03	0.14 ± 0.02	--
Zn(Tb)S/Hg	1.36 ± 0.08	0.42 ± 0.08	0.17 ± 0.01	9.15 ± 0.41	3.94 ± 0.37	0.80 ± 0.04	0.20 ± 0.04	--
Zn(Tb)S/Cd	2.64 ± 0.44	1.14 ± 0.31	0.20 ± 0.01	5.62 ± 0.19	2.04 ± 0.70	1.21 ± 0.05	0.13 ± 0.06	0.09 ± 0.01
Zn(Tb)S/Ca	2.90 ± 0.01	2.41 ± 0.44	0.18 ± 0.02	1.19 ± 0.30	2.76 ± 0.19	2.75 ± 0.19	0.24 ± 0.05	0.27 ± 0.05
Zn(Tb)S/Mg	2.70 ± 0.14	2.48 ± 0.15	0.17 ± 0.02	0.86 ± 0.05	3.00 ± 0.07	2.96 ± 0.81	0.23 ± 0.04	0.29 ± 0.06
Zn(Tb)S/Na	2.44 ± 0.41	2.70 ± 0.16	0.14 ± 0.01	0.52 ± 0.09	2.86 ± 0.40	3.24 ± 0.28	0.25 ± 0.08	0.32 ± 0.07

Zn(Tb)S/K	2.18 ± 0.54	2.47 ± 0.09	0.18 ± 0.03	0.50 ± 0.06	4.12 ± 0.63	3.43 ± 0.02	0.34 ± 0.06	0.33 ± 0.01
------------------	-------------	-------------	-------------	-------------	-------------	-------------	-------------	-------------

B. Reverse Cation Exchange.

Table S7. Elemental Composition of the NPs from Reverse Cation Exchange.

System	Zn		S		
ZnS	41.70 ± 0.40		58.30 ± 0.80		
ZnS/M/Zn	Zn		S		M
ZnS/Pb/Zn	97.88 ± 0.07		0.90 ± 0.07		1.22 ± 0.01
ZnS/Hg/Zn	98.32 ± 0.33		0.86 ± 0.05		0.82 ± 0.08
ZnS/Cd/Zn	95.12 ± 0.43		4.30 ± 0.40		0.58 ± 0.03
System	Zn	Tb	S		
Zn(Tb)S	39.40 ± 0.50	5.8 ± 0.42	54.80 ± 0.60		
Zn(Tb)S/M/Zn,Tb	Zn	Tb	S	M	
Zn(Tb)S/Pb/Zn,Tb	96.17 ± 0.21		1.83 ± 0.09	0.85 ± 0.08	1.15 ± 0.04
Zn(Tb)S/Hg/Zn,Tb	98.11 ± 0.04		0.51 ± 0.01	0.92 ± 0.02	0.46 ± 0.06
Zn(Tb)S/Cd/Zn,Tb	94.18 ± 1.00		0.97 ± 0.33	4.30 ± 0.38	0.58 ± 0.08

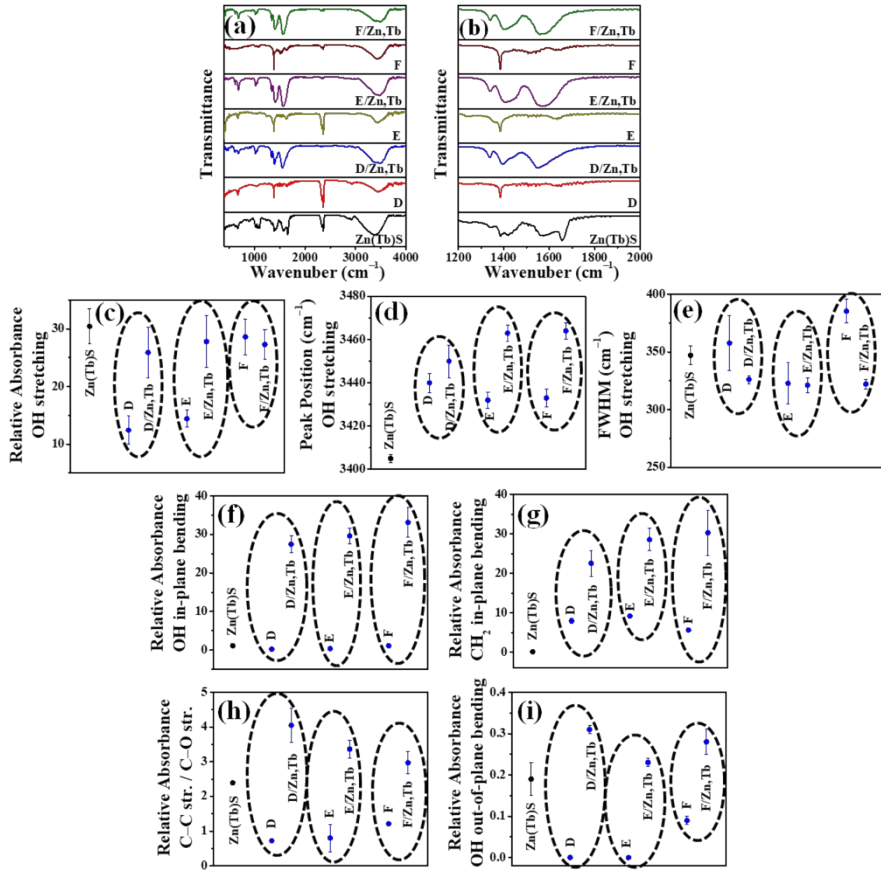


Figure S15. FTIR spectra from the Zn^{2+} and Tb^{3+} re-addition experiments to the $[\text{Zn}(\text{Tb})\text{S}] : [\text{M}^{n+}] = 1:1$ [$\text{M}^{n+} = \text{Pb}^{2+}, \text{Hg}^{2+}, \text{Cd}^{2+}$] NPs are shown in panel (a). Panel (b) shows an enlarged view of the spectral region comprising OH and CH_2 in-plane bending vibrations. In the spectra D, E, and F refer to the $\text{Zn}(\text{Tb})\text{S}/\text{Pb}$, $\text{Zn}(\text{Tb})\text{S}/\text{Hg}$, and $\text{Zn}(\text{Tb})\text{S}/\text{Cd}$ NPs, respectively. Panels (c) – (e), (f) – (g), (h) – (i) summarize the IR spectral trends of OH stretching, OH in-plane bending, CH_2 in-plane bending, C–C stretching / C–O stretching, OH out-of-plane bending, respectively.

Table S8. Spectral Parameter of OH Stretching Band of ZnS, Reversible ZnS/M and Zn(Tb)S, Reversible Zn(Tb)S/M ($M^{n+} = Pb^{2+}, Hg^{2+}, Cd^{2+}$) NPs.

System	Relative absorbance $\int [I_{OH\ st.}]dv / \int [I_{CH_2\ st.}]dv$	Spectral peak position (cm^{-1})	FWHM (cm^{-1})
ZnS	32.65 ± 1.51	3407 ± 2	335 ± 5
ZnS/Pb	11.47 ± 2.82	3436 ± 6	354 ± 13
ZnS/Pb/Zn	24.01 ± 2.19	3456 ± 4	322 ± 3
ZnS/Hg	13.65 ± 2.35	3422 ± 6	348 ± 18
ZnS/Hg/Zn	24.31 ± 4.45	3462 ± 2	324 ± 3
ZnS/Cd	31.94 ± 6.05	3426 ± 4	368 ± 3
ZnS/Cd/Zn	27.00 ± 4.81	3454 ± 2	317 ± 9
<hr/>			
Zn(Tb)S	30.44 ± 3.04	3405 ± 2	347 ± 8
Zn(Tb)S/Pb	12.43 ± 2.46	3440 ± 5	358 ± 24
Zn(Tb)S/Pb/Zn,Tb	25.91 ± 4.35	3450 ± 8	326 ± 4
Zn(Tb)S/Hg	14.41 ± 1.48	3432 ± 4	323 ± 18
Zn(Tb)S/Hg/Zn,Tb	27.80 ± 4.48	3463 ± 4	321 ± 6
Zn(Tb)S/Cd	28.60 ± 3.08	3433 ± 4	385 ± 10
Zn(Tb)S/Cd/Zn,Tb	27.28 ± 2.60	3464 ± 4	322 ± 4

Table S9. Comparison of Methylenes Stretching IR Absorption Band Spectral Properties in the Different Systems Investigated from Reverse Cation Exchange.

System	$I[v_{as}[CH_2]] / I[v_s[CH_2]]$	$\int [I[v_{as}[CH_2]]dv / \int [I[v_s[CH_2]]dv]$	FWHM [$v_{as}[CH_2]$] (cm^{-1})	FWHM [$v_s[CH_2]$] (cm^{-1})
ZnS	5.40 ± 0.05	5.00 ± 0.47	47 ± 5	38 ± 6
ZnS/Pb	2.75 ± 0.32	2.60 ± 0.68	33 ± 2	21 ± 1
ZnS/Pb/Zn	2.41 ± 0.25	2.20 ± 0.41	33 ± 2	25 ± 3
ZnS/Hg	2.47 ± 0.13	1.98 ± 0.14	37 ± 5	26 ± 5
ZnS/Hg/Zn	2.58 ± 0.18	1.28 ± 0.02	32 ± 3	21 ± 2
ZnS/Cd	2.78 ± 0.30	2.91 ± 0.86	44 ± 1	27 ± 2
ZnS/Cd/Zn	3.15 ± 0.46	2.50 ± 0.53	43 ± 2	25 ± 5
<hr/>				
Zn(Tb)S	5.35 ± 1.12	6.22 ± 1.22	35 ± 1	26 ± 4
Zn(Tb)S/Pb	3.00 ± 0.42	2.76 ± 0.57	33 ± 2	22 ± 3
Zn(Tb)S/Pb/Zn,Tb	3.08 ± 0.09	2.60 ± 0.06	25 ± 1	11 ± 1
Zn(Tb)S/Hg	2.12 ± 0.45	1.45 ± 0.50	36 ± 5	25 ± 7
Zn(Tb)S/Hg/Zn,Tb	3.15 ± 0.42	2.38 ± 0.78	35 ± 3	17 ± 3
Zn(Tb)S/Cd	2.25 ± 1.20	4.10 ± 0.60	31 ± 4	21 ± 4
Zn(Tb)S/Cd/Zn,Tb	2.91 ± 0.29	3.66 ± 0.60	26 ± 1	12 ± 1

Table S10. Comparison of (a) OH in-plane bending, (b) CH₂ in-plane bending, (c) C–C str. / C–O str., and (d) OH out-of-plane bending IR Absorption Band Spectral Properties in the Different Systems Investigated from Reverse Cation Exchange.

System	Relative absorbance $\int [I_{OH \text{ in-plane bending}}] dv / \int [I_{CH_2 \text{ str.}}] dv$	Relative absorbance $\int [I_{CH_2 \text{ in-plane bending}}] dv / \int [I_{CH_2 \text{ str.}}] dv$	Relative absorbance $\int [I_{\text{C-C str. / C-O str.}}] dv / \int [I_{CH_2 \text{ str.}}] dv$	Relative absorbance $\int [I_{OH \text{ out-of-plane bend.}}] dv / \int [I_{CH_2 \text{ str.}}] dv$
ZnS	1.43 ± 0.22	0.08 ± 0.03	2.64 ± 0.21	0.22 ± 0.07
ZnS/Pb	0.27 ± 0.02	8.96 ± 0.20	1.01 ± 0.30	--
ZnS/Pb/Zn,Tb	22.96 ± 3.92	19.15 ± 1.63	3.21 ± 0.19	0.29 ± 0.02
ZnS/Hg	0.41 ± 0.14	8.18 ± 0.90	1.19 ± 0.43	--
ZnS/Hg/Zn,Tb	33.93 ± 4.55	32.43 ± 6.21	3.79 ± 0.41	0.30 ± 0.03
ZnS/Cd	1.30 ± 0.28	6.58 ± 0.75	1.60 ± 0.39	0.26 ± 0.04
ZnS/Cd/Zn,Tb	33.00 ± 3.10	31.20 ± 1.87	2.51 ± 0.61	0.22 ± 0.01
Zn(Tb)S	1.15 ± 0.18	0.09 ± 0.01	2.39 ± 0.03	0.19 ± 0.04
Zn(Tb)S/Pb	0.25 ± 0.01	7.90 ± 0.66	0.72 ± 0.03	--
Zn(Tb)S/Pb/Zn,Tb	27.45 ± 2.21	22.53 ± 3.32	4.05 ± 0.50	0.31 ± 0.01
Zn(Tb)S/Hg	0.42 ± 0.08	9.15 ± 0.41	0.80 ± 0.04	--
Zn(Tb)S/Hg/Zn,Tb	29.60 ± 2.09	28.56 ± 2.86	3.36 ± 0.25	0.23 ± 0.01
Zn(Tb)S/Cd	1.14 ± 0.31	5.62 ± 0.19	1.21 ± 0.05	0.09 ± 0.01
Zn(Tb)S/Cd/Zn,Tb	33.12 ± 3.80	30.27 ± 5.77	2.97 ± 0.32	0.28 ± 0.03

Photoluminescence Spectroscopy. Photoluminescence spectra were acquired by using a Horiba Fluorolog 3-22 photoluminescence spectrometer. The NPs were excited at 280 nm to collect the emission spectra. Excitation and emission slits were maintained at 4 nm spectral resolution, respectively. Emission spectra were corrected for lamp and detector response. All the measurements were performed at room temperature. Emission quantum yields were measured using a relative method,¹² and using coumarin 153 dissolved in methanol ($\Phi = 0.42$)³³ as a reference standard.

In order to address how NP's inter band gap energy levels get affected during the reverse cation exchange reaction, we wish to compare the photoluminescence emission spectra in the ZnS, ZnS / M [M = Pb / Hg / Cd] and ZnS / M [M = Pb / Hg / Cd] / Zn NPs. Panel (a) in Figure S16 shows the corresponding spectra. The spectra in the reverse exchanged NPs indeed differs significantly compared to that of in the initial ZnS NPs, suggesting that the contributions from inter band gap energy levels and the electron – hole pair recombination resulting the broad emission in the reverse exchanged NPs is different.

Reverse exchanged NPs generally in cases from completely cation exchanged NPs, [NPs] : [Pb²⁺] / [Hg²⁺] = 1:1, show a remarkably red shifted emission with much narrower spread in energies. These trends can be corroborated with the non identical behavior between the initial and reverse exchanged NPs observed from IR measurements. To this end, it is important to iterate that in the report by Alivisatos and co-workers ¹ on the CdSe to Ag₂Se to CdSe transformation, they also observed that in the reverse exchanged retrieved CdSe NPs in addition to the core emission of CdSe a red shifted emission appears. These observations further stress on the fact that probably the reverse exchanged NPs generally offer a way to develop a unique nanostructure that is not identical to the original nanostructure used to initiate the cation exchange process.

Panel (b) in Figure S16 visualizes the different deactivation pathways, which includes intrinsic ZnS [Zn and S vacancies (V_{Zn}, V_S) and Zn and S at interstitial positions (I_{Zn}, I_S)], ³⁴ NP's surface states and residual cation based inter band gap energy levels. For this, only representative energy levels from contribution of residual cation are shown. The role of residual cations to influence the emission properties of nanomaterials in cation exchange reaction is demonstrated by Alivisatos and co-workers. ³⁵ To this end, we stress that this exercise of comparing the photoluminescence emission was just to examine whether the NP emission reverts back identically to the original unmodified ZnS NPs, and qualitatively correlate that with the non-identical spectral retrieval of 1-TG IR absorption spectral characteristics following the reverse cation exchange.

Decrease in ZnS based broad emissions were actually observed in the initially exchanged NPs (curves with dashed lines in Figure S16), however, this emission is indeed largely retrieved following the reverse exchange reaction (curves with solid lines in Figure S16). The emission quantum yields of ZnS, and reverse exchanged ZnS/Pb/Zn, ZnS/Hg/Zn and ZnS/Cd/Zn NPs were found to be $(2.10 \pm 0.30) \times 10^{-4}$, $(1.83 \pm 0.01) \times 10^{-4}$, (1.87 ± 0.01)

$\times 10^{-4}$, and $(1.90 \pm 0.19) \times 10^{-4}$, respectively. A small amount of residual cations following the reverse exchange reaction with an atomic percent of 0.80 ± 0.32 might be associated with this. However, the red shift in the emission band position following the reverse exchange and the near similar emission quantum yield values irrespective of the identity of the residual cations can be taken as an indication with intrinsic modulation of ZnS inter band gap energy levels being primarily responsible to govern the spectral outcome.

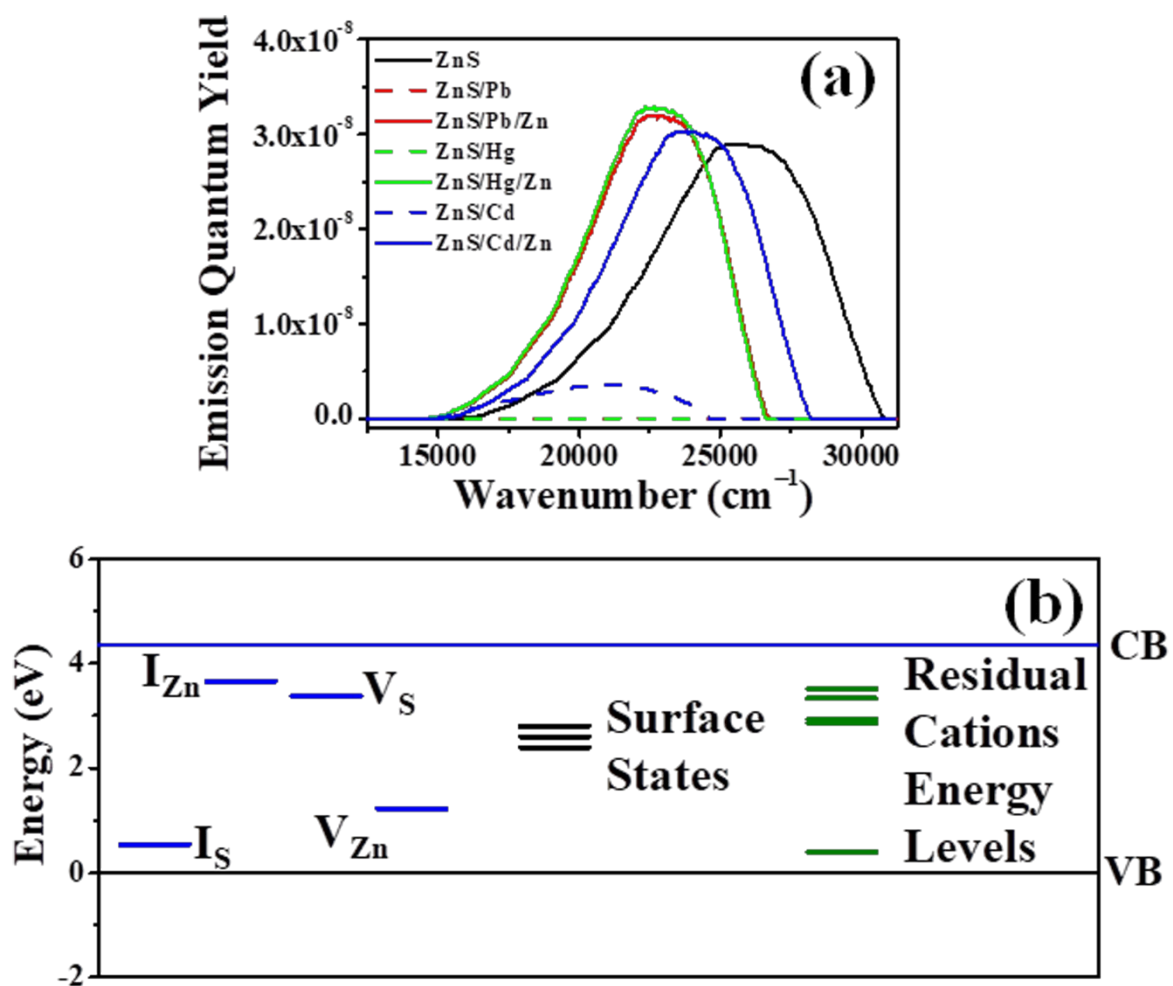


Figure S16. Photoluminescence spectra of ZnS, ZnS/M [$M^{n+} = Pb^{2+}, Hg^{2+}, Cd^{2+}$] and ZnS/M/Zn [$M^{n+} = Pb^{2+}, Hg^{2+}, Cd^{2+}$] NPs are shown in panel (a). Areas under the spectra are normalized to the emission quantum yields. Panel (b) shows the energy levels that can contribute to the relaxation pathways.

C. $[Zn(Tb)S] : [Pb^{2+}] = 1:10^{-5} - 1:10$: A Case Study.

Table S11. Spectral Parameters of OH Stretching Band of $[Zn(Tb)S] : [Pb^{2+}] = 1:10^{-5} - 1:10$.

System	Relative absorbance $\int [I_{OH\ st.}]dv / \int [I_{CH_2\ st.}]dv$	Spectral peak position (cm^{-1})	FWHM (cm^{-1})
1-TG	7.53 ± 0.14	3400 ± 1	455 ± 20
Zn(Tb)S	30.44 ± 3.04	3405 ± 2	347 ± 8
[Zn(Tb)S]:[Pb²⁺]			
1:10⁻⁵	26.21 ± 4.49	3405 ± 4	372 ± 5
1:10⁻⁴	25.51 ± 4.10	3405 ± 6	370 ± 8
1:10⁻³	30.06 ± 9.01	3405 ± 3	368 ± 14
1:10⁻²	23.24 ± 2.11	3404 ± 4	367 ± 9
1:10⁻¹	18.89 ± 3.31	3417 ± 6	360 ± 8
1:1	12.43 ± 2.46	3440 ± 4	358 ± 24
1:10	14.43 ± 6.48	3440 ± 7	331 ± 26

Table S12. Comparison of IR Spectral Properties in the Methylene Stretching Region in the Different Concentrations of $[Zn(Tb)S] : [Pb^{2+}] = 1:10^{-5} - 1:10$.

System	$I[v_{as}[CH_2]] / I[v_s[CH_2]]$	$\int [I[v_{as}[CH_2]]dv / \int [I[v_s[CH_2]]dv]$	FWHM [$v_{as}[CH_2]$] (cm^{-1})	FWHM [$v_s[CH_2]$] (cm^{-1})
1-TG	2.23 ± 0.11	2.76 ± 0.11	46 ± 4	30 ± 1
Zn(Tb)S	5.35 ± 1.12	6.22 ± 1.22	35 ± 1	26 ± 4
[Zn(Tb)S]:[Pb²⁺]				
1:10⁻⁵	5.01 ± 1.13	7.06 ± 0.20	39 ± 4	26 ± 4
1:10⁻⁴	4.41 ± 1.11	4.71 ± 1.15	39 ± 1	28 ± 4
1:10⁻³	6.56 ± 2.08	3.74 ± 0.83	39 ± 1	28 ± 3
1:10⁻²	3.10 ± 0.57	2.15 ± 0.76	41 ± 1	29 ± 3
1:10⁻¹	2.87 ± 0.97	3.13 ± 1.10	40 ± 1	30 ± 4
1:1	3.00 ± 0.42	2.76 ± 0.57	33 ± 2	22 ± 3
1:10	1.13 ± 0.19	1.79 ± 0.01	31 ± 3	21 ± 4

Table S13. Relative Absorbance of (a) OH in-plane bending, (b) CH₂ in-plane bending, (c) C–C str. / C–O str., and (d) OH out-of-plane bending of $[Zn(Tb)S] : [Pb^{2+}] = 1:10^{-5} - 1:10$.

System	Relative absorbance $\int [I_{OH\ in-plane\ bending}]dv / \int [I_{CH_2\ str.}]dv$	Relative absorbance $\int [I_{CH_2\ in-plane\ bending}]dv / \int [I_{CH_2\ str.}]dv$	Relative absorbance $\int [I_{C-C\ str.\ / C-O\ str.}]dv / \int [I_{CH_2\ str.}]dv$	Relative absorbance $\int [I_{OH\ out-of-plane\ bending}]dv / \int [I_{CH_2\ str.}]dv$
1-TG	0.55 ± 0.06	0.16 ± 0.01	0.96 ± 0.16	0.14 ± 0.01
Zn(Tb)S	1.15 ± 0.18	0.09 ± 0.01	2.39 ± 0.03	0.19 ± 0.04
[Zn(Tb)S]:[Pb²⁺]				
1:10⁻⁵	1.05 ± 0.11	0.11 ± 0.02	3.34 ± 0.68	0.18 ± 0.02
1:10⁻⁴	1.03 ± 0.16	0.10 ± 0.01	3.23 ± 0.39	0.16 ± 0.01
1:10⁻³	1.01 ± 0.16	0.13 ± 0.04	3.01 ± 0.27	0.14 ± 0.01
1:10⁻²	0.98 ± 0.02	0.12 ± 0.03	2.83 ± 0.49	0.14 ± 0.02
1:10⁻¹	0.33 ± 0.02	7.53 ± 0.74	2.39 ± 0.33	0.09 ± 0.01
1:1	0.25 ± 0.01	7.90 ± 0.66	0.72 ± 0.03	--
1:10	--	17.97 ± 0.37	--	--

References

1. D. H. Son, S. M. Hughes, Y. Yin and A. P. Alivisatos, *Science*, 2004, **306**, 1009-1012.
2. R. D. Robinson, B. Sadtler, D. O. Demchenko, C. K. Erdonmez, L.-W. Wang and A. P. Alivisatos, *Science*, 2007, **317**, 355-358.
3. B. Sadtler, D. O. Demchenko, H. Zheng, S. M. Hughes, M. G. Merkle, U. Dahmen, L.-W. Wang and A. P. Alivisatos, *J. Am. Chem. Soc.*, 2009, **131**, 5285-5293.
4. D. Mocatta, G. Cohen, J. Schattner, O. Millo, E. Rabani and U. Banin, *Science*, 2011, **332**, 77-81.
5. S. Acharya and N. Pradhan, *J. Phys. Chem. C*, 2011, **115**, 19513-19519.
6. A. Jaiswal, S. S. Ghosh and A. Chattopadhyay, *Langmuir*, 2012, **28**, 15687-15696.
7. I. R. Pala and S. L. Brock, *ACS Appl. Mater. Interfaces*, 2012, **4**, 2160-2167.
8. A. Sahu, M. S. Kang, A. Kompch, C. Notthoff, A. W. Wills, D. Deng, M. Winterer, C. D. Frisbie and D. J. Norris, *Nano Lett.*, 2012, **12**, 2587-2594.
9. J. Liu, Q. Zhao, J.-L. Liu, Y.-S. Wu, Y. Cheng, M.-W. Ji, H.-M. Qian, W.-C. Hao, L.-J. Zhang, X.-J. Wei, S.-G. Wang, J.-T. Zhang, Y. Du, S.-X. Dou and H.-S. Zhu, *Advanced Materials*, 2015, **27**, 2753-2761.
10. G. H. Debnath, S. Rudra, A. Bhattacharyya, N. Guchhait and P. Mukherjee, *Journal of Colloid and Interface Science*, 2019, **540**, 448-465.
11. S. Rudra, G. H. Debnath and P. Mukherjee, *RSC Adv.*, 2018, **8**, 18093-18108.
12. S. Rudra, M. Bhar and P. Mukherjee, *J. Phys. Chem. C*, 2019, **123**, 29445-29460.
13. B. J. Beberwyck and A. P. Alivisatos, *J. Am. Chem. Soc.*, 2012, **134**, 19977-19980.
14. K. Miszta, D. Dorfs, A. Genovese, M. R. Kim and L. Manna, *ACS Nano*, 2011, **5**, 7176-7183.
15. H. Li, M. Zanella, A. Genovese, M. Povia, A. Falqui, C. Giannini and L. Manna, *Nano Lett.*, 2011, **11**, 4964-4970.
16. H. Li, R. Brescia, M. Povia, M. Prato, G. Bertoni, L. Manna and I. Moreels, *J. Am. Chem. Soc.*, 2013, **135**, 12270-12278.
17. L. D. Trizio, H. Li, A. Casu, A. Genovese, A. Sathya, G. C. Messina and L. Manna, *J. Am. Chem. Soc.*, 2014, **136**, 16277-16284.
18. K. Sooklal, B. S. Cullum, S. M. Angel and C. J. Murphy, *J. Phys. Chem.*, 1996, **100**, 4551-4555.
19. A. V. Isarov and J. Chrysochoos, *Langmuir*, 1997, **13**, 3142-3149.
20. A. W. Wills, M. S. Kang, K. M. Wentz, S. E. Hayes, A. Sahu, W. L. Gladfelter and D. J. Norris, *J. Mater. Chem.*, 2012, **22**, 6335-6342.
21. S. Deka, K. Miszta, D. Dorfs, A. Genovese, G. Bertoni and L. Manna, *Nano Lett.*, 2010, **10**, 3770-3776.
22. V. Lesnyak, C. George, A. Genovese, M. Prato, A. Casu, S. Ayyappan, A. Scarpellini and L. Manna, *ACS Nano*, 2014, **8**, 8407-8418.
23. E. Groeneveld, L. Witteman, M. Lefferts, X. Ke, S. Bals, G. V. Tendeloo and C. d. M. Donega, *ACS Nano*, 2013, **7**, 7913-7930.
24. X. Zhong, Y. Feng, Y. Zhang, Z. Gu and L. Zou, *Nanotechnology* 2007, **18**, 385606 (385606pp).
25. E. Groeneveld, S. v. Berkum, M. M. v. Schooneveld, A. Gloter, J. D. Meeldijk, D. J. v. d. Heuvel, H. C. Gerritsen and C. d. M. Donega, *Nano Lett.*, 2012, **12**, 749-757.
26. C. Bothe, A. Kornowski, H. Tornatzky, C. Schmidtke, H. Lange, J. Maultzsch and H. Weller, *Angew. Chem. Int. Ed.*, 2015, **54**, 14183-14186.
27. P. Mukherjee, R. F. Sloan, C. M. Shade, D. H. Waldeck and S. Petoud, *J. Phys. Chem. C*, 2013, **117**, 14451-14460.

28. L. Chen, J. Zhang, S. Lu, X. Ren and X. Wang, *Chemical Physics Letters*, 2005, **409**, 144-148.
29. X. Zhong, M. Han, Z. Dong, T. J. White and W. Knoll, *J. Am. Chem. Soc.*, 2003, **125**, 8589-8594.
30. X. Zhong, Z. Zhang, S. Liu, M. Han and W. Knoll, *J. Phys. Chem. B*, 2004, **108**, 15552-15559.
31. M. Casavola, M. A. v. Huis, S. Bals, K. Lambert, Z. Hens and D. Vanmaekelbergh, *Chem. Mater.*, 2012, **24**, 294-302.
32. B. J. Beberwyck, Y. Surendranath and A. P. Alivisatos, *J. Phys. Chem. C*, 2013, **117**, 19759-19770.
33. J. E. Lewis and M. Maroncelli, *Chem. Phys. Lett.*, 1998, **282**, 197-203.
34. D. Denzler, M. Olschewski and K. Sattler, *J. Appl. Phys.*, 1998, **84**, 2841-2845.
35. P. K. Jain, B. J. Beberwyck, L.-K. Fong, M. J. Polking and A. P. Alivisatos, *Angew. Chem. Int. Ed.*, 2012, **51**, 2387-2390.